KSME International Journal, Vol. 16 No. 2, pp. 175~181, 2002

Separation of Isochromatics and Isoclinics from Photoelastic Fringes in a Circular Disk by Phase Measuring Technique

Tae Hyun Baek*, Myung Soo Kim
College of Engineering, Kunsan National University, Chonbuk 573-701, Korea
Yoshihau Morimoto, Motoharu Fujigaki
Department of Opto-Mechatronics, Faculty of Systems Engineering, Wakayama University, Wakayama 640-8510, Japan

A new polariscope system involving two rotating optical elements and a digital camera for whole field fringe analysis allows automated data to be acquired quickly and efficiently. The developed phase measuring technique that uses eight images through a circular polariscope is presented for the digital measurement of isochromatics and isoclinics, respectively, from photoelastic fringes in a circular disk under diametric compression. Isochromatics can directly be obtained using wrapped isoclinic phases calculated by the arc tangent operator which is the four-quadrant operator from $-\pi$ to π. It is not required to unwrap isoclinic phases for the calculations of isochromatics. Unwrapped isoclinics are directly determined from isochromatic parameters. Distributions of digitally determined isoclinics are in close agreement to manual measurements. The errors which would appear in unwrapping process of isoclinics can be avoided in the determination of isochromatics.

Key Words : Photoelasticity, Isochromatics, Isoclinics, Fringe, Phase Measuring Technique, Whole Field Stress Analysis, Digital Image Processing

1. Introduction

Photoelasticity is one of the most widely used techniques for the whole field stress analysis in the experimental mechanics. The method of photoelasticity allows one to obtain the principal stress directions and principal stress differences in a model. The principal stress directions and the principal stress differences are provided by isoclinics and isochromatics, respectively. Conventionally, the principal stress directions are measured manually by rotating the polarizer and analyzer of a plane polariscope at the same time. This measurement is very tedious and time consuming in whole field analysis. It is not possible to separate isoclinics from photoelastic fringes by conventional photoelastic technique. There have been several methods devised for automatic measurements of photoelastic fringes, and these include half-fringe photoelasticity (Voloshin & Burger, 1983), phase measuring technique (Asundi, 1993; Baek et al., 2000a; Quiroga & Gonzales-Cano, 1997), and several other methods (Baek & Burger, 1991; Baek et al., 2000b; Morimoto et al., 1994) using digital imaging system. Among them the phase measuring technique, which can be used to obtain isoclinic and isochromatic parameters from a combination of several images taken by the rotation of optical components, is promising for the whole field analysis.

This paper presents a new method to separate isochromatics and isoclinics from photoelastic fringes through a circular polariscope and photoelastic experiments are performed to verify the new method. The method used in this study is an eight-step phase measuring technique.

* Corresponding Author,
E-mail : thbaek@kunsan.ac.kr
TEL : +82-63-469-4714; **FAX** : +82-63-469-4727
School of Mechanical Engineering, Kunsan National University, #68, Miryong-Dong, Kunsan, Chonbuk, 573-701, Korea. (Manuscript **Received** March 20, 2001; **Revised** December 1, 2001)

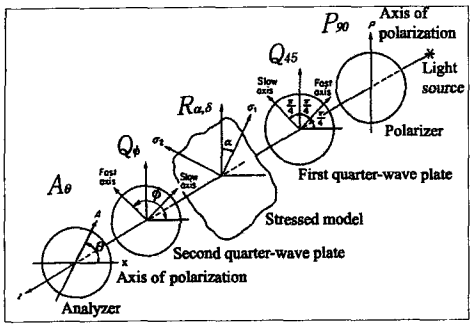

Fig. 1 Optical arrangement of a circular polariscope

2. Method of Analysis

The optical arrangement to separate isoclinics and isochromatics from photoelastic fringes is a circular polariscope set-up in Fig. 1. In Fig. 1, P, Q, R and A stand for polarizer, quarter-wave plate, retarder (stressed model) and analyzer, respectively. The orientation of the element is written by a subscript which means the angle between the polarizing axis and the horizontal x axis. For example, P_{90} indicates a polarizer whose transmission axis is perpendicular to the chosen x axis. $R_{\alpha,\delta}$ stands for the stressed sample taken as a retardation δ and whose fast axis is at an angle α with the x axis. Therefore by $P_{90}Q_{45}R_{\alpha,\delta}Q_\phi A_\theta$ we mean: ① a polarizer at 90°, ② a quarter-wave plate with fast axis at 45°, ③ a specimen as retardation δ and whose fast axis is at an angle α with the x axis, ④ a quarter-wave plate with fast axis at ϕ, and ⑤ an analyzer at θ.

With the Jones calculus for the arrangement of $P_{90}Q_{45}R_{\alpha,\delta}Q_\phi A_\theta$ in Fig. 1, the components of electric field in light along and perpendicular to the analyzer axis (E_x, E_y) are given as (Theocaris & Gdoutos, 1979)

$$\begin{pmatrix}E_x\\E_y\end{pmatrix}=\begin{bmatrix}\cos^2\theta & \sin\theta\cos\theta\\ \sin\theta\cos\theta & \sin^2\theta\end{bmatrix}\times \begin{bmatrix}i\cos^2\phi+\sin^2\phi & (i-1)\sin\phi\cos\phi\\ (i-1)\sin\phi\cos\phi & i\sin^2\phi+\cos^2\phi\end{bmatrix}\times \begin{bmatrix}e^{i\delta}\cos^2\alpha+\sin^2\alpha & (e^{i\delta}-1)\sin\alpha\cos\alpha\\ (e^{i\delta}-1)\sin\alpha\cos\alpha & e^{i\delta}\sin^2\alpha+\cos^2\alpha\end{bmatrix}\times \left(\frac{i+1}{2}\right)\begin{bmatrix}1 & i\\ i & 1\end{bmatrix}\begin{pmatrix}0\\1\end{pmatrix}ke^{i\omega t} \quad (1)$$

where $i=\sqrt{-1}$, θ and ϕ are the angles that the analyzer and the second quarter-wave plate form with the reference x axis, respectively. The symbols of k and ω are the amplitude and the angular frequency of the light vector, respectively.

Table 1 Optical arrangements and their intensity equations

No.	Arrangement	Output Intensity
1	$P_{90}Q_{45}R_{\alpha,\delta}Q_{45}A_{-45}$	$I_1=K(1+\cos 2\alpha\sin\delta)$
2	$P_{90}Q_{45}R_{\alpha,\delta}Q_{-45}A_{45}$	$I_2=K(1-\cos 2\alpha\sin\delta)$
3	$P_{90}Q_{45}R_{\alpha,\delta}Q_{-45}A_0$	$I_3=K(1-\cos\delta)$
4	$P_{90}Q_{45}R_{\alpha,\delta}Q_{45}A_0$	$I_4=K(1+\cos\delta)$
5	$P_{90}Q_{45}R_{\alpha,\delta}Q_0A_0$	$I_5=K(1+\sin 2\alpha\sin\delta)$
6	$P_{90}Q_{45}R_{\alpha,\delta}Q_{90}A_{90}$	$I_6=K(1-\sin 2\alpha\sin\delta)$
7	$P_{90}Q_{45}R_{\alpha,\delta}Q_0A_{45}$	$I_7=K(1-\cos\delta)$
8	$P_{90}Q_{45}R_{\alpha,\delta}Q_{90}A_{45}$	$I_8=K(1+\cos\delta)$

$$I=\overline{E_x}\cdot E_x+\overline{E_y}\cdot E_y \quad (2)$$

In Eq. (2), I is the output light intensity, and $\overline{E_x}$, $\overline{E_y}$ are the complex conjugates of E_x and E_y, respectively.

After the simple operation of Eq. (1) by Eq. (2), the output intensity of the circular polariscope for the arrangement $P_{90}Q_{45}R_{\alpha,\delta}Q_\phi A_\theta$ is given by

$$I=K[1-\sin 2(\theta-\phi)\cos\delta-\sin 2(\phi-\alpha)\cos 2(\theta-\phi)\sin\delta] \quad (3)$$

where K is a proportional constant, i.e., the maximum light intensity emerging from the analyzer. For phase measuring technique, the angle α and the relative retardation δ indicating the direction and the difference of principal stresses, respectively, are the parameters to be obtained.

For this study, eight images whose intensity equations in Table 1 are used. For instance, output intensity I_1 of No. 1 arrangement in Table 1 can be obtained from Eq. (3) when $\theta=45°$ and $\phi=45°$ in Fig. 1 are used. The optical arrangements of Table 1 are similar to those of Ref. (Quiroga & Gonzales-Cano, 1997). However, the polarizer and the first quarter wave plate as in Fig. 1 and Table 1 are fixed with angles 90 and 45 degrees, respectively, from the x axis in these arrangements. These arrangements are simple to use and take short time in actual data-acqui-

sition.

The equations shown in Table 1 are used for the calculations of isoclinic α and fractional fringe order δ as (Baek et al., 2001),

$$\alpha=\frac{1}{2}\tan^{-1}\left(\frac{I_5-I_6}{I_1-I_2}\right) \tag{4}$$

$$\delta=\tan^{-1}\left[\frac{(I_1-I_2)\cos 2\alpha+(I_5-I_6)\sin 2\alpha}{\frac{1}{2}\{(I_4-I_3)+(I_8-I_7)\}}\right] \tag{5}$$

3. Simulation Test

A feasibility study using computer simulation is done to separate isoclinics and isochromatics from photoelastic fringes of a circular disk under diametric compression (Baek et al., 2001). The radius and the thickness of the disk used in the simulation test are 3.81 cm (1.5 in.) and 0.476 cm (3/16 in.), respectively. Diametrical compression load, P=26.7 N (6 lb), is applied to the disk. Material fringe constant, f_σ=5.254 N/cm (3.0 lb/in.), is used. From the given conditions, theoretical value of isochromatic δ is related to two principal stress components, σ_1 and σ_2, as in Eq. (6). On the other hand, theoretical isoclinc angle α can be calculated by Eq. (7) using stress components, σ_x, σ_y, and τ_{xy}(Baek et al., 2001).

$$\delta=\frac{2\pi t}{f_\sigma}(\sigma_1-\sigma_2) \tag{6}$$

$$\alpha=\frac{1}{2}\tan^{-1}\left\{\frac{\tau_{xy}}{\frac{\sigma_x-\sigma_y}{2}}\right\} \tag{7}$$

From the simulated eight images of the circular disk (Baek et al., 2001), isoclinic phase map using Eq. (4) can be obtained as in Figs. 2(a) and 2 (b). Figure 2(a) is processed by the use of atan, where phase jumps near the top and the bottom loading points occur beyond $\alpha=\pi/4$. However, Fig. 2(b) is obtained by the use of atan2. In this case, phase jumps occur at every position where isochromatic is changed. The function denoted by atan is the two-quadrant arc tangent operator and only calculates the ranges from $-\pi/2$ to $\pi/2$. On the other hand, the function of atan2 from the ANSI standard for the C language is the four -quadrant operator and calculates the ranges from $-\pi$ to π.

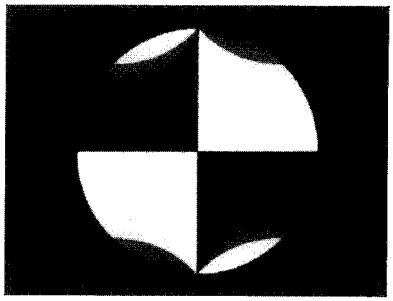

(a)

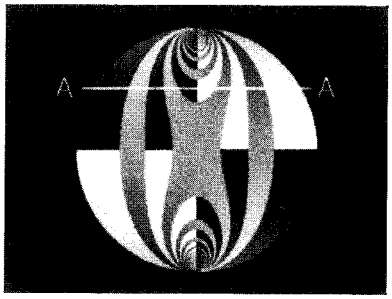

(b)

Fig. 2 Simulation of a disk under diametric compression: Phase maps of isoclinics using the operators of (a) atan and (b) atan2

Figures 2(a) and 2(b) are used to yield isochromatic phase map as in Figs. 3(a) and 3 (b), respectively. Note that the phase map of isochromatics of Fig. 3(a) is inverted near the top and the bottom of the disk where the isoclinic angle is beyond $\alpha=\pi/4$. The isochromatic phase map in Fig. 3(b) is different from that of Fig. 3 (a). Phase jump near the top and the bottom of the disk is not observed in Fig. 3(b).

Due to the ambiguity of arc tangent, phase jump occurs when a resultant value exceeds the specified range, i.e., the range of $-\pi\sim\pi$ when the atan2 function is used. This is called as a wrapped phase. In order to get continuous distributions and/or physical quantities, the values at the phase jump should be connected by means of unwrapping procedure. Figure 4 shows wrapped and unwrapped phase distributions of isochromatics along a line A-A across the middle point of the upper half disk indicated in Fig. 3 (a). On the other hand, Fig. 5 shows wrapped and unwrapped isochromatic phase distributions

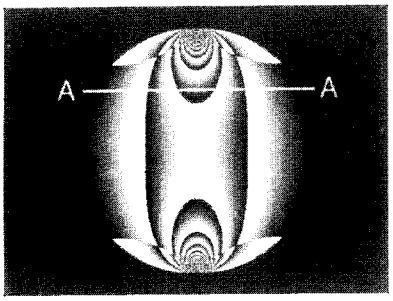

(a)

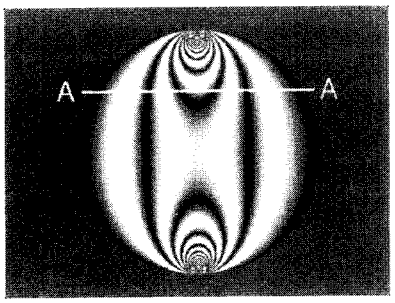

(b)

Fig. 3 Phase maps of isochromatics using (a) Fig. 2 (a) and (b) Fig. 2(b)

along the same line A-A as indicated in Fig. 3 (b). The distributions of wrapped phase in Fig. 5 are different from those of Fig. 4. Those differences may be due to use of wrapped isoclinics in Fig. 2(b). However, it can be observed that the unwrapped phase distributions of Fig. 4 agree exactly with the unwrapped phase distributions of Fig. 5. In Fig. 6, the distributions of wrapped isoclinic phase map along the horizontal line A -A is shown. As shown in Fig. 6, the phases of isoclinics are changed when $I_1=I_2=I_5=I_6$ in Table 1, which occur when $\delta=0$, π, 2π, etc. The phase changes of isoclinics in Fig. 6 can be eliminated after unwrapping isochromatic phase, which represents δ as in Fig. 5. The distributions of unwrapped isoclinic phase are shown in Fig. 7, and they are exactly agreed to those of theories calculated by Eq. (7). However, big errors occur at or near the centers of isochromatic fringes. These errors can be easily recognized and taken off by simple image processing. All the results in Figs. 4 through 7 are calculated from the simulated images of the circular disk. It can be verified that the procedure for the separation of isochromatics and isoclinics from photoelastic fringes used in the simulation is valid.

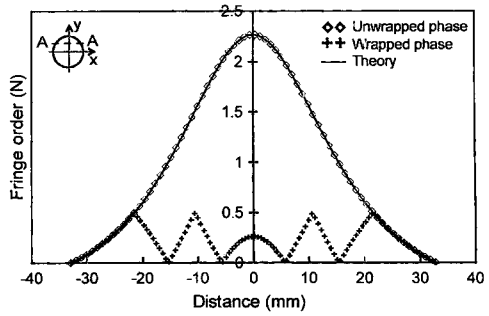

Fig. 4 Distributions of unwrapped and wrapped isochromatic phase map along line A-A of Fig. 3(a)

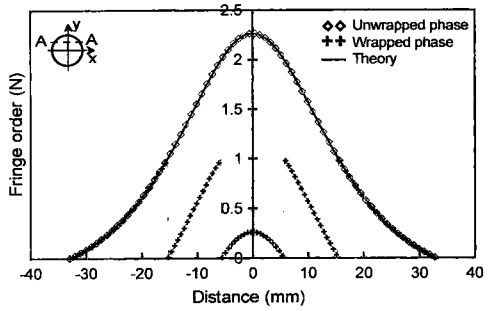

Fig. 5 Distributions of unwrapped and wrapped isochromatic phase map along line A-A of Fig. 3(b)

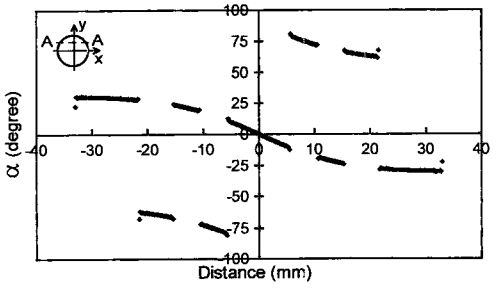

Fig. 6 Distributions of wrapped isoclinic phase map along line A-A of Fig. 2(b)

4. Experiment

To assess the practical use of the developed method in this work, a stress-frozen disk under diametric compression, 45.2 mm in diameter and 4.0 mm thick made of epoxy, is used. Material

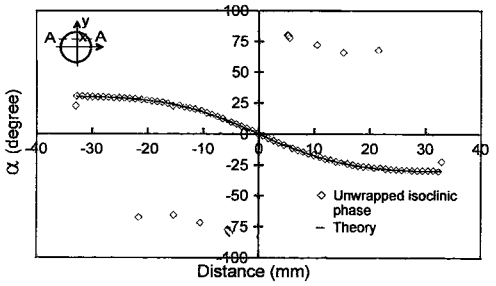

Fig. 7 Distributions of unwrapped isoclinic phase map along line A-A of Fig. 2(b) using unwrapped isochromatics of Fig. 5

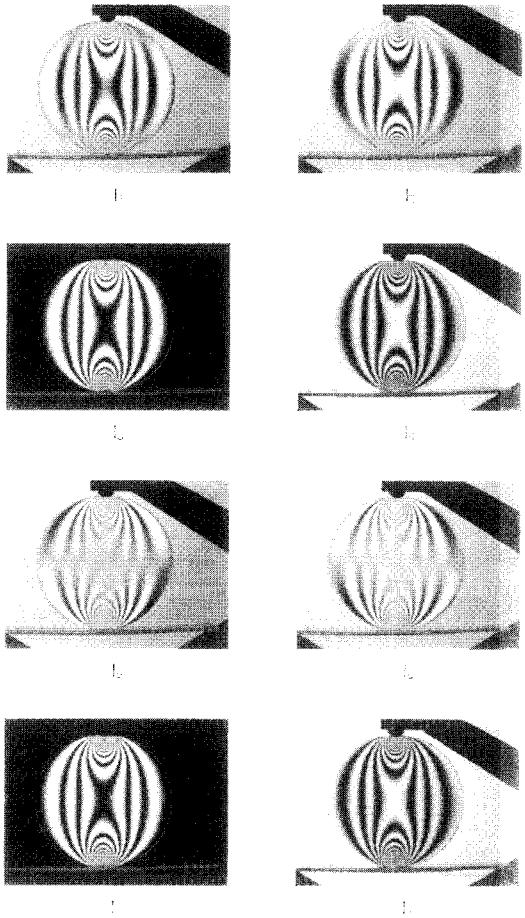

Fig. 8 Eight images obtained from the optical arrangements of Table 1

fringe value and applied load at the stress freezing point are f_σ=0.3517 kN/m and P=36.15 N, respectively. Pixel numbers, which are used for digitization, are 640×480. The grey level of each

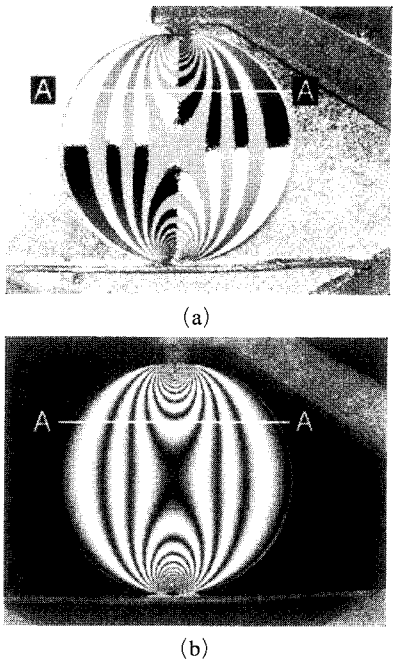

(a)

(b)

Fig. 9 Wrapped phases of (a) isoclinics and (b) isochromatics

pixel ranges from 0 to 255. A diffused-light polariscope with four separate elements which can be rotated independently is setup. The light source used in this experiment is monochromatic light of sodium lamp. Eight images of Table 1 are digitized as shown in Fig. 8 using a CCD camera. Isoclinic phase map using Eq. (2) is shown in Fig. 9(a). The function of atan2 is used in the calculation of Eq. (2). This isoclinic phase map of Fig. 9(a) is directly used for the calculation of isochromatic phase as shown in Fig. 9(b).

5. Results and Discussions

In order to check the distributions of isochromatics quantitatively, unwrapped phase in Fig. 10 is obtained from the wrapped phase of isochromatics along a line A-A across the middle point of the upper half disk as shown in Fig. 9 (b). Note that the wrapped phases of isochromatics in Fig. 10 are directly obtained from the wrapped isoclinic phases shown in Fig. 9(a). As mentioned earlier, wrapped isoclinic phases are calculated by the arc tangent operator,

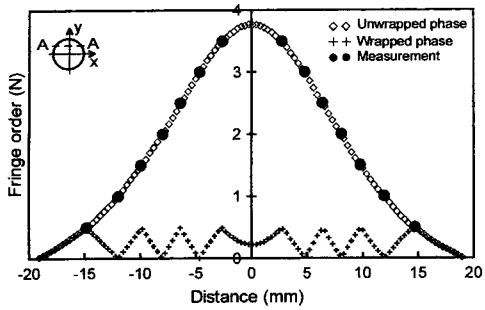

Fig. 10 Unwrapped and wrapped isochromatic phase distributions along line A-A indicated in Fig. 9(b)

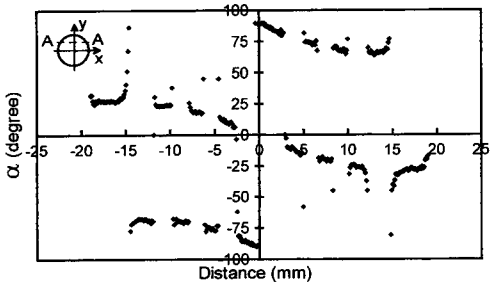

Fig. 11 Wrapped isoclinic phase distributions along line A-A indicated in Fig. 9(a)

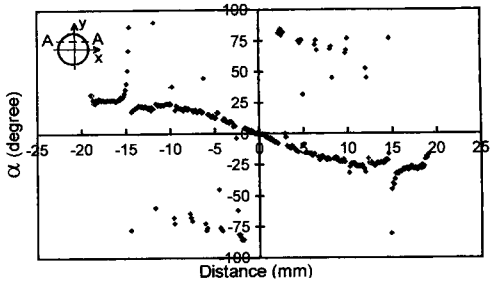

Fig. 12 Unwrapped isoclinic phase distributions along line A-A indicated in Fig. 9(a)

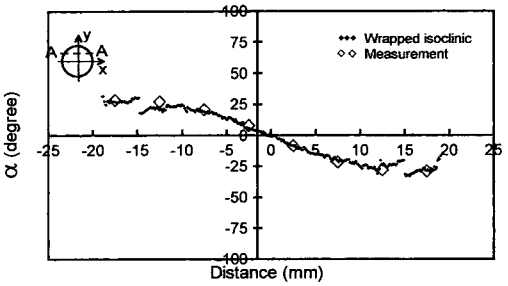

Fig. 13 Comparisons of digitally determined isoclinic distributions and manual measurements along line A-A indicated in Fig. 9(a)

atan2, which is the four-quadrant operator and calculates those from $-\pi$ to π. Generally, unwrapping of wrapped isoclinics should be prerequisite to get wrapped isochromatic phases. In this research, it is not required to unwrap isoclinic phase for the calculations of isochromatics. Also, it is possible to exclude possible errors due to numerical calculation and/or digitization for unwrapping isoclinics. The experimental results obtained from unwrapped isochromatics are exactly agreed to the manual measurements at the fringe centers as shown in Fig. 10.

Figure 11 shows the wrapped isoclinic distributions along a line A-A in Fig. 9(a). The unwrapped isoclinic phases of Fig. 12 can be obtained by using unwrapped isochromatics of Fig. 10. In other words, unwrapping isoclinics are done after unwrapping isochromatics. Unexpected big errors occur at or near the centers of isochromatics. These errors can easily be recognized and eliminated by means of appropriate image processing. Results of the digitally determined isoclinics along a line A-A are compared with those determined from the manual measurements in Fig. 13. Again, it can be observed that digitally determined unwrapped isoclinics are close to manual measurements.

6. Conclusions

From the results presented in the preceeding simulation and experiments, the following significant conclusions can be drawn:

(1) Isochromatics can directly be obtained using wrapped isoclinic phases calculated by the arc tangent operator, atan2, which is the four-quadrant operator and calculates those from $-\pi$ to π. It is not required to unwrap isoclinic phase for the calculations of isochromatics. The experimental results obtained from unwrapped isochromatics are exactly agreed to the manual measurements at the fringe centers.

(2) Unwrapped isoclinics are obtained using

isochromatic parameters, and the distributions of digitally determined unwrapped isoclinic phases are in close agreement to manual measurements.

In most of previous researches (Quiroga & Gonzales-Cano, 1997 ; Ramesh & Ganapathy, 1996), unwrapping of wrapped isoclinics must be done before the isochromatic calculations. However, in this research, it is not required to unwrap isoclinic phase to get isochromatic phase. This can lead to exclude some possible errors due to numerical calculation and/or digitization for unwrapping isoclinics. In digitally measured unwrapped isoclinics, unexpected big errors occur at or near the centers of isochromatics. These errors can easily be recognized and eliminated by means of appropriate image processing.

Acknowledgement

This work was supported by grant No. R02-2000-00294 from the Korea Science & Engineering Foundation.

References

Voloshin, A. S. and Burger, C. P, 1983, "Half-fringe Photoelasticity: A New Approach to Whole-field Stress Analysis," *Experimental Mechanics*, Vo. 23, pp. 304~313.

Asundi, A., 1993, "Phase Shifting in Photoelasticity," *Experimental Techniques*, Vol. 7, No. 1, pp. 19~23.

Baek, T. H., Kim, M. S. and Kim, S. I., 2000a, "Stress Analysis of a Curved Beam Plate by using Photoelastic Fringe Phase Shifting Technique," *Transactions of the Korean Society of Mechanical Engineers A*, Vol. 24, No. 9, pp. 2313~2318.

Quiroga, J. A. and Gonzales-Cano, A., 1997, "Phase Measuring Algorithm for Extraction of Isochromatis of Photoelastic Fringe Patterns," *Applied Optics*, Vo. 36, No. 2, pp. 8397~8402.

Baek, T. H. and Burger, C. P., 1991, "Accuracy Improvement Technique for Measuring Stress Intensity Factors in Photoelastic Experiment," *KSME International Journal*, Vol. 5, No. 1, pp. 22~27.

Baek, T. H., Kim, M. S., Rhee, J. and Rowlands, R. E., 2000b, "Hybrid Stress Analysis of Perforated Tensile Plates using Multiplied and Sharpened Photoelastic Data and Complex-Variable Techniques," *JSME International Journal, Series A: Solid Mechanics and Material Engineering*, Vol. 43, No. 4, pp. 327~333.

Morimoto, Y., Morimoto, Y., Jr., and Hayashi, T., 1994, "Separation of Isochromatics and Isoclinics using Fourier Transform," *Experimental Techniques*, pp. 13~17.

Theocaris, P. S. and Gdoutos, E. E., 1979, *Matrix Theory of Photoelasticity*, Springer-Verlag, pp. 50~55.

Baek, T. H., Kim, M. S. and Cho, S. H., 2001, "Simulation of Separating Isoclinics and Isochromatics from Photoelastic Fringes of a Disk using 8-step Phase Shifting Methodology," *Journal of the Korean Society for Nondestructive Testing*, Vol. 21, No. 2, pp. 189~196.

Ramesh, K. and Ganapathy, V., 1996, "Phase-shifting Methodologies in Photoelastic Analysis-The Application of Jones Calculus," *Journal of Strain Analysis*, Vol. 31, No. 1, pp. 423~432.